

# Electron-electron interaction strength in ferromagnetic nickel determined by spin-polarized positron annihilation

Hubert Ceeh,<sup>1</sup> Josef-Andreas Weber,<sup>1</sup> Peter Böni,<sup>1</sup> Michael Leitner,<sup>2</sup> Diana Benea,<sup>3,4</sup> Liviu Chioncel,<sup>5,6</sup> Dieter Vollhardt,<sup>6</sup> Hubert Ebert,<sup>3</sup> Jan Minár,<sup>3,7</sup> and Christoph Hugenschmidt<sup>1,2</sup>

<sup>1</sup>*Technische Universität München, Lehrstuhl E21,  
James-Franck Straße, 85748 Garching, Germany*

<sup>2</sup>*Heinz Maier-Leibnitz Zentrum (MLZ), Technische Universität München, Lichtenbergstraße 1, 85748 Garching, Germany*

<sup>3</sup>*Chemistry Department, University Munich, Butenandstraße 5-13, 81377 München, Germany*

<sup>4</sup>*Faculty of Physics, Babes-Bolyai University, Kogălniceanu 1, 400084 Cluj-Napoca, Romania*

<sup>5</sup>*Augsburg Center for Innovative Technologies, University of Augsburg, D-86135 Augsburg, Germany*

<sup>6</sup>*Theoretical Physics III, Center for Electronic Correlations and Magnetism,  
Institute of Physics, University of Augsburg, 86135 Augsburg, Germany*

<sup>7</sup>*New Technologies - Research Center, University of West Bohemia, Univerzitní 8, 306 14 Pilsen, Czech Republic*

(Dated: January 14, 2015)

The two-photon momentum distribution of annihilating electron-positron pairs in ferromagnetic nickel (Ni) was determined by measuring the spin-polarized two-dimensional angular correlation of annihilation radiation (ACAR). The spectra were compared with theoretical results obtained within LDA+DMFT, a combination of the local density approximation (LDA) and the many-body dynamical mean-field theory (DMFT). The self-energy describing the electronic correlations in Ni is found to make important anisotropic contributions to the momentum distribution which are not present in LDA. Based on a detailed comparison of the theoretical and experimental results the strength of the local electronic interaction  $U$  in ferromagnetic Ni is determined as  $2.0 \pm 0.1$  eV.

The electronic properties of many narrow-band materials, such as the  $d$ -shell transition-metal series and their compounds, cannot be explained within a one-electron picture, because there exist strong correlations between electrons in the partially filled  $d$  band [1–4]. Such systems are therefore better described by multi-band models such as the Hubbard or Anderson-type lattice model. In these models the *local* Coulomb repulsion  $U$  is assumed to be the dominant interaction between the electrons. The “Hubbard” parameter  $U$  was originally introduced for single-band models [5, 6] and is defined as the Coulomb-energy required to place two electrons on the same site:  $U = E(d^{n+1}) + E(d^{n-1}) - 2E(d^n)$ . Here  $E(d^n)$  represents the total energy of a system for which  $n$  electrons fill a given  $d$ -shell on a given atom. In multi-band systems  $U$  takes the form of an interaction matrix.

The Hubbard model and related lattice models are able to explain important general features of correlated electrons, but they cannot describe the physics of real materials in any detail. Namely, for an approach to be realistic it must take into account the explicit electronic and lattice structure of the systems. Here the LDA+DMFT approach has led to great progress in the understanding of correlated electron materials [3, 7–11]. LDA+DMFT is a computational scheme where the local density approximation (LDA) or the generalized-gradient approximation (GGA) provide the material dependent input (orbitals and hopping parameters), while DMFT [2, 12] solves the interacting local many-body problem originating from the local Hubbard interaction  $U$  and Hund’s rule coupling  $J$ . The results can be compared with experimental data obtained, for example, by photoemission spec-

troscopy. In particular, this technique measures spectral functions, i.e., the imaginary part of a one-particle Green function, and thus determines correlation induced shifts of the spectral weight. This allows one to estimate the local Hubbard interaction  $U$  of a material, say, Ni. Indeed, most investigations on the electronic structure of Ni relied on photoemission spectroscopy [13, 14]. Braun *et al.* [15] demonstrated the importance of local correlations in Ni by exploiting the magnetic circular dichroism in bulk sensitive soft X-ray photoemission measurements. One of the dominant correlation effects observed in the photoemission data for Ni is the satellite peak situated at 6 eV below the Fermi level [16, 17]. This feature is not captured by LDA, but is well explained by LDA+DMFT [18]. LDA+DMFT also reproduces the correct width of the occupied  $3d$  bands and the exchange splitting [18]. A fundamental difficulty concerning the interpretation of photoemission data is the fact that they involve an interaction of photons with matter. This makes the determination of a parameter such as the Hubbard  $U$  quite difficult. Namely, it is not only necessary to describe the excitation process, but also the propagation of the photoelectrons in the material as well as the process of detection itself. Therefore the experimental data, and the values of the interaction parameters derived from them, will be strongly influenced by the surface of a sample.

In this Letter we discuss an alternative experimental technique to determine the local Coulomb parameter  $U$ , involving *positrons*. In contrast to photoemission experiments positron spectroscopy experiments measure a two-particle Green function. Since there are no physical processes except the electron-positron annihilation, positron

spectroscopy does not suffer from the above-mentioned difficulties faced by photoelectron spectroscopy. As a consequence the magnitude of  $U$  deduced from positron spectroscopy is much less influenced by external effects (e.g., surfaces), which are difficult to control. Here we show that by combining experimental results of the spin-polarized two-dimensional angular correlation of annihilation radiation (2D-ACAR) with LDA+DMFT computations it is possible to assess the strength of the electronic interactions in Ni quite unambiguously. We mea-

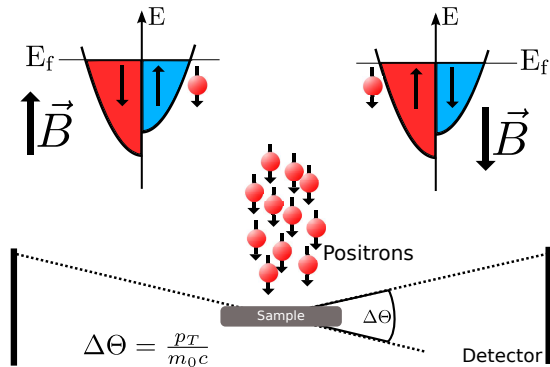


Figure 1. (Color Online) Schematic principle of spin polarized 2D-ACAR: In electron-positron annihilation the singlet configuration is preferred for majority or minority spin electrons if the magnetization of the sample is parallel or anti-parallel to the emission direction of the positrons.

sured spin-resolved two-dimensional projections of the two-photon momentum distribution (TPMD) in magnetic fields up to 1.1 T at room temperature. The field was applied parallel and anti-parallel, respectively, relative to the crystallographic  $\langle 110 \rangle$  orientation of the sample which coincides with the emission direction of the positrons (i.e., the polarization direction of the positron beam). The  $\beta^+$  spectrum of  $^{22}\text{Na}$ , which served as positron source, has an end-point energy of 545 keV with a mean energy of about 215 keV. This corresponds to a beam polarization of 74 % for forward emission. Both, the positron back reflection in the source capsule and the magnetic guiding field, lower the net polarization of the beam, which was determined as 34.4(5) % in a separate experiment. Although the positron undergoes multiple scattering during thermalization [19–21] the polarization of the positrons remains essentially unchanged until the moment of annihilation. Quantum electrodynamics predicts the annihilation rate in the triplet configuration to be significantly smaller ( $1/1115$ ) than that in the singlet configuration [22, 23]. When an external magnetic field is applied parallel ( $\uparrow\uparrow$ ) or anti-parallel ( $\uparrow\downarrow$ ) to the emission direction the positrons will therefore annihilate predominantly with electrons from the majority or the minority spin directions, respectively (see Fig. 1). The result of a magnetic 2D-ACAR measurement can be expressed

as [23]

$$\Delta N_{\text{exp}}(p_x, p_y) = N_{\uparrow\uparrow}(p_x, p_y) - N_{\uparrow\downarrow}(p_x, p_y) \quad (1)$$

where  $N_{\uparrow(\downarrow)}(p_x, p_y)$  is the number of coincident photon counts measured with the positron spin aligned parallel ( $\uparrow$ ) and anti-parallel ( $\downarrow$ ), respectively, to the applied field. For a detailed description of the experimental technique we refer to Refs. [24–26]. Spin-polarized 2D-ACAR is one of the few experimental methods that can probe the momentum distribution of the electrons in the bulk with respect to the spin direction. It was successfully applied to elemental Ni [27] and other materials [28–31]. In Fig. 2 we present the spin-difference of the 2D-ACAR measurement of Ni. In each spectrum an excess of 250 million counts was collected, and the data were corrected for the momentum sampling function. Before subtraction, the spectra  $N_{\uparrow\uparrow}$  and  $N_{\uparrow\downarrow}$  were normalized to an equal amount of counts. A renormalization due to  $3\gamma$  decay was omitted since the corresponding correction in the case of Ni [23] is negligible compared to the statistical noise. The 4-fold symmetry is clearly observed in agreement with the study of Manuel *et al.* [27]. It should be noted that the difference spectrum (see inset of Fig. 2) is anisotropic, i.e., the signal is more intense along the  $\Gamma - X - \Gamma$  direction than along the  $\Gamma - L - \Gamma$  direction.

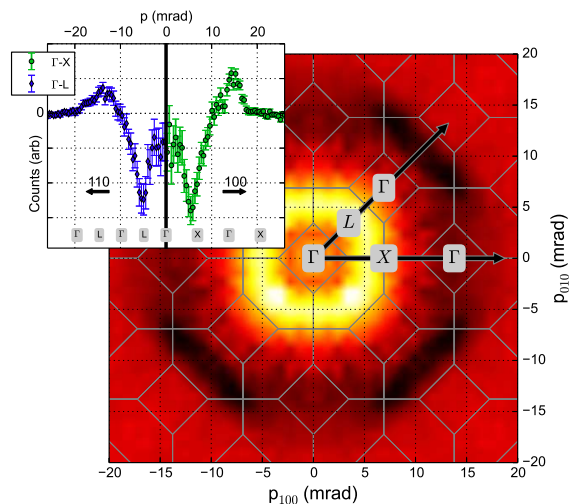


Figure 2. (Color Online) 2D-ACAR difference spectra  $\Delta N_{\text{exp}}(p_x, p_y)$  obtained when the magnetic field is reversed, with the integration along the  $\langle 001 \rangle$  direction,  $p_x = \langle 100 \rangle$  and  $p_y = \langle 010 \rangle$ . The inset illustrates the anisotropy of the difference spectra between two directions in momentum space.

To represent the difference spectra  $\Delta N_{\text{exp}}(p_x, p_y)$  in  $\mathbf{k}$ -space we apply the magnetic Lock-Crisp-West (LCW) back-folding procedure. In practice this amounts to taking the difference of the individual spin-resolved LCW-projections [32] since the LCW-procedure is nothing but a linear transformation. According to this scheme, first proposed by Biasini *et al.* [33, 34], effects due to the

electron-positron interaction, known as enhancement, are cancelled out. This proves to be particularly advantageous as no complete microscopic description for the enhancement problem is available. Several recipes have been discussed in the literature [35–41] and have also been consequently applied for Ni [42, 43]. Hence, the only parameter in this analysis is a uniform scale factor, which is obtained by fitting the amplitude of theoretical spectra to experimental data.

The theoretical analysis requires the knowledge of the two-particle electron-positron Green function, describing the probability amplitude for an electron and a positron propagating between two different space-time points. In view of the fact that experiments performed on Ni [43–45] show no significant enhancement effects, we factorize the two-particle Green function into a product of electronic and positronic Green functions. Thereby Coulomb interaction induced correlation effects between the annihilating particles are neglected. At the same time correlations between the *electrons* are explicitly included in the DMFT.

Electronic structure calculations were performed with the spin-polarized relativistic Korringa-Kohn-Rostoker (SPR-KKR) method [46]. For LDA computations the exchange-correlation potentials parametrized by Vosko, Wilk and Nusair [47] were used with a lattice parameter of 3.52 Å. To include the electronic correlations, a charge and self-energy self-consistent LDA+DMFT scheme was employed, which is based on the KKR approach [48] and where the impurity problem is solved with a spin-polarized  $T$ -matrix fluctuation exchange (SPTF) method [10, 49]. This impurity solver is fully rotationally invariant even in the multi-orbital version and is reliable when the interaction  $U$  is smaller than the bandwidth, a condition which is fulfilled in the case of Ni. In this LDA+DMFT framework the electron-positron momentum density  $\rho_\sigma(\mathbf{p})$  is computed directly from the two-particle Green function in the momentum representation. The neglect of electron-positron correlations corresponds to the factorization of the two-particle Green function in real space. In the numerical implementation the position-space integrals for the “auxiliary” Green function  $G_{\sigma\sigma'}(\mathbf{p}_e, \mathbf{p}_p)$  obtained within LDA or LDA+DMFT, respectively, are performed as integrals over unit cells:

$$G_{\sigma\sigma'}^\alpha(\mathbf{p}_e, \mathbf{p}_p, E_e, E_p) = \frac{1}{N\Omega} \int d^3\mathbf{r} \int d^3\mathbf{r}' \phi_{\mathbf{p}_e\sigma}^{e\dagger}(\mathbf{r}) \text{Im} G_{e+}^\alpha(\mathbf{r}, \mathbf{r}', E_e) \phi_{\mathbf{p}_p\sigma}^e(\mathbf{r}') \phi_{\mathbf{p}_p\sigma'}^{p\dagger}(\mathbf{r}) \text{Im} G_{p+}(\mathbf{r}, \mathbf{r}', E_p) \phi_{\mathbf{p}_p\sigma'}^p(\mathbf{r}'), \quad (2)$$

where  $\alpha = \text{LDA or LDA+DMFT}$ , and  $(\mathbf{p}_e, \sigma)$ , and  $(\mathbf{p}_p, \sigma')$  are the momenta and spin of electron and positron, respectively. Here  $G_{\sigma\sigma'}^\alpha$  is computed for each energy point on the complex energy contour, providing

the electron-positron momentum density:

$$\rho_\sigma^\alpha(\mathbf{p}) = -\frac{1}{\pi} \int dE_e G_{\sigma\sigma'}^\alpha(\mathbf{p}_e, \mathbf{p}_p, E_e, E_p). \quad (3)$$

Integration over positron energies  $E_p$  is not required, since only the ground state is considered, and  $\sigma' = -\sigma$  at the annihilation. The momentum carried off by the photons is equal to that of the two particles up to a reciprocal lattice vector, reflecting the fact that the annihilation takes place in a crystal. Hence an electron with wave vector  $\mathbf{k}$  contributes to  $\rho_\sigma^\alpha(\mathbf{p})$  not only at  $\mathbf{p} = \mathbf{k}$  (normal process) but also at  $\mathbf{p} = \mathbf{k} + \mathbf{K}$ , with  $\mathbf{K}$  a vector of the reciprocal lattice (Umklapp process). The experimental spin-difference spectra  $\Delta N_{exp}(p_x, p_y)$  can be compared with the computed difference in the integrated momentum densities of Eq. 3:

$$\Delta N_{theo}^\alpha(p_x, p_y) = \int dp_z [\rho_\uparrow^\alpha(\mathbf{p}) - \rho_\downarrow^\alpha(\mathbf{p})]. \quad (4)$$

In Fig. 3 we show the measured  $\Delta N_{exp}(p_x, p_y)$  and the theoretical  $\Delta N_{theo}^\alpha(p_x, p_y)$  LCW-folded difference spectra for different values of  $U$ . It is clearly seen that with in-

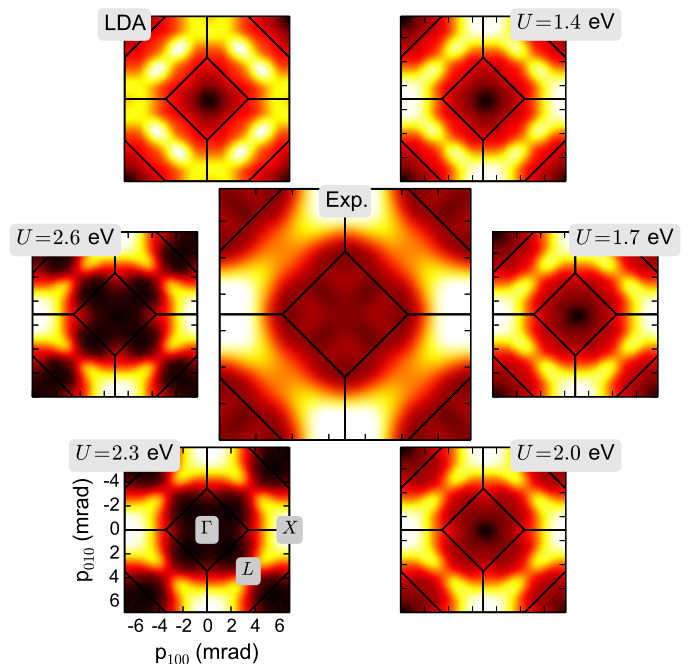


Figure 3. (Color Online) Experimental magnetic LCW spectrum (center) compared to theoretical spectra computed for different values of the local Coulomb parameter  $U$  in the range from 1.4 to 2.3 eV.

creasing  $U$  a gap opens at the L-points of the Brillouin zone. This gap is associated with the necks in the FS of Ni. Apparently LDA underestimates the density at the X-point, while the density near the L-point is overestimated. In the LDA+DMFT calculation the highest

density is found at the X-point, similar to the experimental data. However, the structure connecting the X and L-points is less pronounced in the experimental data than in the LDA+DMFT results. Obviously the local interaction (see e.g. [15]) pushes the  $d$ -bands below the Fermi energy, whereby the  $X_2$  hole pocket obtained in LDA disappears. This also greatly changes the calculated anomalous Hall effect of Ni [50, 51].

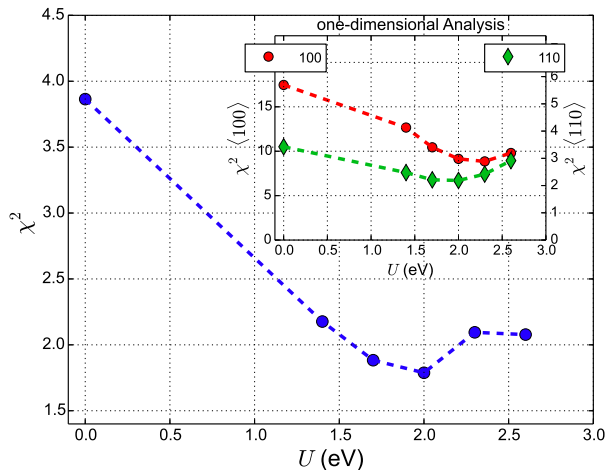


Figure 4. (Color Online) Least square fit analysis ( $\chi^2$ ) between LDA+DMFT calculations and experimental data as a function of the Hubbard  $U$  for the 2D data. Higher  $U$  values correspond to stronger electron-electron correlations. A pronounced minimum of  $\chi^2$  is found for  $U = 2.0$  eV. The inset shows the results for the 1D data. (The dotted lines act as a guide to the eye.)

In order to derive the value of the local Coulomb interaction parameter  $U$  we performed a least square fit analysis of the measured data with the LDA+DMFT calculations (Fig. 3). The result is summarized in Fig. 4. A distinct minimum in  $\chi^2$  is found at  $U = 2.0$  eV. The 1D data are shown in the inset of Fig. 4. Although the spin difference spectra along different directions in momentum space are not the same, the  $\chi^2$  curves have their minima in the same region around  $U = 2.0$  eV of the Hubbard interaction. The loss of information in the twice-integrated 1D data is indicated by a larger  $\chi^2$  value. Interpolating the data in Fig. 4 with higher order polynomials allows us to estimate the systematic error in the position of the absolute minimum as  $\pm 0.1$  eV. The resulting value  $U = 2.0 \pm 0.1$  eV supports the conclusion of recent measurements of the Compton scattering profiles [52, 53] where values of 2.0 eV and 2.3 eV for  $U$  were reported.

To conclude, we have shown that spin-polarized 2D-ACAR is a powerful tool to investigate the electronic structure of ferromagnetic systems especially when combined with LDA+DMFT calculations. Here the strength of magnetic 2D-ACAR becomes apparent: the higher in-

formation content of the two-dimensional data compared to twice-integrated one-dimensional data from Compton scattering. We found strong evidence for the existence of electron pockets around the X point which are related to electronic correlation effects. A detailed comparison of the experimental results with electronic structure calculations in the framework of LDA+DMFT allowed us to evaluate the local Coulomb interaction (“Hubbard”  $U$ ) as  $2.0 \pm 0.1$  eV.

This project was funded by the Deutsche Forschungsgesellschaft (DFG) through the Transregional Collaborative Research Center TRR 80 and Research Unit FOR1346. DB acknowledges the DAAD and the CNCS - UEFISCDI(PN-II-ID-PCE-2012-4-0470). JM acknowledge also the CENTEM project (CZ.1.05/2.1.00/03.0088 co-funded by the ERDF).

- 
- [1] M. Imada, A. Fujimori, and Y. Tokura, *Rev. Mod. Phys.* **70**, 1039 (1998).
  - [2] A. Georges, G. Kotliar, W. Krauth, and M. J. Rozenberg, *Rev. Mod. Phys.* **68**, 13 (1996).
  - [3] G. Kotliar and D. Vollhardt, *Phys. Today* **57**, 53 (2004).
  - [4] G. Kotliar, S. Y. Savrasov, K. Haule, V. S. Oudovenko, O. Parcollet, and C. A. Marianetti, *Rev. Mod. Phys.* **78**, 865 (2006).
  - [5] J. Hubbard, *Proc. R. Soc. London* **276**, 238 (1963).
  - [6] M. C. Gutzwiller, *Phys. Rev. Lett.* **10**, 159 (1963).
  - [7] G. Kotliar, S. Y. Savrasov, K. Haule, V. S. Oudovenko, O. Parcollet, and C. A. Marianetti, *Rev. Mod. Phys.* **78**, 865 (2006).
  - [8] K. Held, *Adv. Phys.* **56**, 829 (2007).
  - [9] V. I. Anisimov, A. I. Poteryaev, M. A. Korotin, A. O. Anokhin, and G. Kotliar, *Journal of Physics: Condensed Matter* **9**, 7359 (1997).
  - [10] A. I. Lichtenstein and M. I. Katsnelson, *Phys. Rev. B* **57**, 6884 (1998).
  - [11] K. Held, I. A. Nekrasov, G. Keller, V. Eyert, N. Blümer, A. K. McMahan, R. T. Scalettar, T. Pruschke, V. I. Anisimov, and D. Vollhardt, *physica status solidi (b)* **243**, 2599 (2006).
  - [12] W. Metzner and D. Vollhardt, *Phys. Rev. Lett.* **62**, 324 (1989).
  - [13] P. Aebi, T. J. Kreutz, J. Osterwalder, R. Fasel, P. Schwaller, and L. Schlapbach, *Phys. Rev. Lett.* **76**, 1150 (1996).
  - [14] C. M. Schneider, U. Pracht, W. Kuch, A. Chassé, and J. Kirschner, *Phys. Rev. B* **54**, R15618 (1996).
  - [15] J. Braun, J. Minár, H. Ebert, A. Chainani, J. Miyawaki, Y. Takata, M. Taguchi, M. Oura, and S. Shin, *Phys. Rev. B* **85**, 165105 (2012).
  - [16] J. Sánchez-Barriga, J. Braun, J. Minár, I. Di Marco, A. Varykhalov, O. Rader, V. Boni, V. Bellini, F. Manghi, H. Ebert, M. I. Katsnelson, A. I. Lichtenstein, O. Eriksson, W. Eberhardt, H. A. Dürr, and J. Fink, *Phys. Rev. B* **85**, 205109 (2012).
  - [17] F. J. Himpsel, J. A. Knapp, and D. E. Eastman, *Phys. Rev. B* **19**, 2919 (1979).
  - [18] A. I. Lichtenstein, M. I. Katsnelson, and G. Kotliar,

- Phys. Rev. Lett. **87**, 067205 (2001).
- [19] P. W. Zitzewitz, J. C. Van House, A. Rich, and D. W. Gidley, Phys. Rev. Lett. **43**, 1281 (1979).
  - [20] P. Kubica and A. T. Stewart, Phys. Rev. Lett. **34**, 852 (1975).
  - [21] A. Seeger, J. Major, and F. Banhart, phys. status solidi (a) **102**, 91 (1987).
  - [22] A. Ore and J. Powell, Phys. Rev. **75**, 1696 (1949).
  - [23] S. Berko and A. P. Mills, J. Phys. Colloques **32**, C1 (1971).
  - [24] R. N. West, J. Mayers, and P. A. Walters, J. Phys. E Sci. Instrum. **14**, 478 (1981).
  - [25] H. Ceeh, J. A. Weber, M. Leitner, P. Böni, and C. Hugenschmidt, Rev. Sci. Instr. **84**, 043905 (2013).
  - [26] M. Leitner, H. Ceeh, and J.-A. Weber, New J. Phys. **14**, 123014 (2012).
  - [27] P. Genoud, A. A. Manuel, E. Walker, and M. Peter, J. Phys. Condens. Mat. **3**, 4201 (1991).
  - [28] K. E. H. M. Hanssen and P. E. Mijnaerends, Phys. Rev. B **34**, 5009 (1986).
  - [29] K. E. H. M. Hanssen, P. E. Mijnaerends, L. P. L. M. Rabou, and K. H. J. Buschow, Phys. Rev. B **42**, 1533 (1990).
  - [30] E. A. Livesay, R. West, S. B. Dugdale, G. Santi, and T. Jarlborg, Materials Science Forum **363-365**, 576 (2001).
  - [31] T. D. Haynes, R. J. Watts, J. Laverock, Z. Major, M. A. Alam, J. W. Taylor, J. A. Duffy, and S. B. Dugdale, New Journal of Physics **14**, 035020 (2012).
  - [32] D. G. Lock, V. H. C. Crisp, and R. N. West, J. Phys. F Met. Phys. **3**, 561 (1973).
  - [33] M. Biasini and J. Ruzs, J. Phys. Condens. Mat. **18**, L289 (2006).
  - [34] J. Ruzs and M. Biasini, Phys. Rev. B **75**, 235115 (2007).
  - [35] A. K. Singh and T. Jarlborg, J. Phys. F Met. Phys. **15**, 727 (1985).
  - [36] T. Jarlborg and A. K. Singh, Phys. Rev. B **36**, 4660 (1987).
  - [37] E. Boroński and R. M. Nieminen, Phys. Rev. B **34**, 3820 (1986).
  - [38] J. Laverock, T. D. Haynes, M. A. Alam, and S. B. Dugdale, Phys. Rev. B **82**, 125127 (2010).
  - [39] I. Makkonen, M. M. Ervasti, T. Siro, and A. Harju, Phys. Rev. B **89**, 041105 (2014).
  - [40] G. Kontrym-Sznajd and H. Sormann, Phys. Scripta **89**, 015808 (2014).
  - [41] G. Kontrym-Sznajd, H. Sormann, and E. Boroński, Phys. Rev. B **85**, 245104 (2012).
  - [42] T. J. A.K. Singh, A.A. Manuel, Helv. Phys. Act. **59** (1986).
  - [43] G. Kontrym-Sznajd, H. Stachowiak, W. Wierzchowski, K. Petersen, N. Thrane, and G. Trumpy, Appl. phys. **8**, 151 (1975).
  - [44] P. E. Mijnaerends and R. M. Singru, Phys. Rev. B **19**, 6038 (1979).
  - [45] B. Barbiellini, M. Hakala, M. J. Puska, R. M. Nieminen, and A. A. Manuel, Phys. Rev. B **56**, 7136 (1997).
  - [46] H. Ebert, D. Ködderitzsch, and J. Minár, Rep. Prog. Phys. **74**, 096501 (2011).
  - [47] S. H. Vosko, L. Wilk, and M. Nusair, Can. J. Phys. **58**, 1200 (1980).
  - [48] J. Minár, L. Chioncel, A. Perlov, H. Ebert, M. I. Katsnelson, and A. I. Lichtenstein, Phys. Rev. B **72**, 045125 (2005).
  - [49] L. Pourovskii, M. Katsnelson, and A. Lichtenstein, Phys. Rev. B **72**, 115106 (2005).
  - [50] H.-R. Fuh and G.-Y. Guo, Phys. Rev. B **84**, 144427 (2011).
  - [51] D. Ködderitzsch, K. Chadova, J. Minár, and H. Ebert, New Journal of Physics **15**, 053009 (2013).
  - [52] L. Chioncel, D. Benea, H. Ebert, I. Di Marco, and J. Minár, Phys. Rev. B **89**, 094425 (2014).
  - [53] L. Chioncel, D. Benea, S. Mankovsky, H. Ebert, and J. Minár, Phys. Rev. B **90**, 184426 (2014).